

# Design of an optical device with three functions based on coordinate transformation

Tinghua Li (李廷华)<sup>1</sup>, Ming Huang (黄 铭)<sup>1\*</sup>, Jingjing Yang (杨晶晶)<sup>1</sup>,  
Yun Feng (冯 云)<sup>2</sup>, and Yan Liang (梁 岩)<sup>1</sup>

<sup>1</sup>Wireless Innovation Laboratory, School of Information Science and Engineering,  
Yunnan University, Kunming 650091, China

<sup>2</sup>Radio Monitoring Center of Yunnan, Kunming 650228, China

\*Corresponding author: huangming@ynu.edu.cn

Received April 19, 2013; accepted July 9, 2013; posted online August 28, 2013

Based on two-step coordinate transformation along the radial direction, an optical device with three functions is proposed. The proposed device functions as a transparent device, a vision-enabling internal cloak, and a movement-allowing external cloak. The general expressions of material parameters for the optical device are determined, and each function of the device is confirmed using full-wave simulation. The effect of material loss on device performance is also investigated. Future applications for the proposed device include antenna protection and military stealth.

OCIS codes: 160.1190, 160.3918, 260.2710.

doi: 10.3788/COL201311.091602.

Transformation optics<sup>[1,2]</sup> (TO) is rooted in the ancient subject of electromagnetics and an emerging field that has inspired a review of the foundations of classical electromagnetic theory. TO helps create new paradigms for the arbitrary control of electromagnetic waves using metamaterials. Based on the form invariance of Maxwell's equations under coordinate transformations, TO opens up many possibilities for exploring extraordinary optical phenomena and designing novel functional devices<sup>[3–6]</sup>. The invisibility cloak, perhaps one of the most intriguing TO applications discovered thus far, has attracted considerable attention in recent years<sup>[7–15]</sup>. Two main kinds of TO-based invisibility cloaks are available: internal cloaks<sup>[7–11]</sup> and external cloaks<sup>[12,13]</sup>. The internal cloak can render whatever it covers undetectable by steering waves around an enclosed domain. The object concealed by an internal cloak is “blind” because no external electromagnetic waves can encroach on the hidden area and vice-versa. The external cloak removes the bottleneck of the internal cloak and leaves the hidden object out in the open so that it can see its surroundings. This cloak employs an anti-object to optically cancel the scattered field from the hidden object. However, a strict one-to-one correspondence between the positions of the anti-object and the hidden object is required in an external cloak. Thus, once the position of the anti-object is fixed, the hidden object cannot move freely. After the first experimental demonstration of a TO-based metamaterial internal cloak in 2006<sup>[7]</sup>, intensive studies on TO-based devices with novel functions, such as field rotators, perfect lenses, illusion devices, transparent devices, and electromagnetic cavities, have been conducted<sup>[16–20]</sup>. The scope of TO research has gradually expanded from optics to acoustics<sup>[21]</sup>, elastodynamics<sup>[22]</sup>, plasmonics<sup>[23]</sup>, and even thermodynamics<sup>[24]</sup>. In earlier investigations, all theoretical analyses, numerical simulations, and parameter designs focused mainly on single-function devices. Recently, however, bifunctional devices have been

designed under the theoretical framework of TO<sup>[25–27]</sup>.

In this letter, a proposal based on two-step coordinate transformation is presented to design an optical device with three distinct functions. Firstly, the device can serve as a transparent device to protect antennas or other radio equipment without affecting their performance. Secondly, the device functions as a traditional internal cloak that hides objects from view. Thirdly, the device exhibits the beneficial characteristics of a traditional external cloak and allows the hidden object to move freely within the device. Full-wave simulation by the finite-element method is performed to verify the performance of the proposed device. The proposed strategy has potential applications in antenna protection, and the device obtained effectively compensates for the insufficiencies of traditional internal and external cloaks. The results of this work could result in a wider range of applications beyond that of normal invisibility cloaks.

TO fully uses the form-invariance of Maxwell's equations under a spatial coordinate transformation to establish the equivalence between metric transformations and changes in material parameters. According to this theory, the general relationship of material parameters between original and transformed spaces under a cylindrical coordinate system can be written as<sup>[8,28]</sup>

$$\varepsilon_r/\varepsilon_0 = \mu_r/\mu_0 = f(r)/rf'(r), \quad (1a)$$

$$\varepsilon_\phi/\varepsilon_0 = \mu_\phi/\mu_0 = rf'(r)/f(r), \quad (1b)$$

$$\varepsilon_z/\varepsilon_0 = \mu_z/\mu_0 = f'(r)f(r)/r, \quad (1c)$$

where  $\varepsilon_r$ ,  $\varepsilon_\phi$ ,  $\varepsilon_z$  and  $\mu_r$ ,  $\mu_\phi$ ,  $\mu_z$  are the permittivity and permeability of the transformed space, respectively. Here,  $\varepsilon_0$  and  $\mu_0$  respectively denote the permittivity and permeability of the original space. The original space is assumed to be free space. The transformation equation between the transformed space and the original space is  $f(r)$ , and  $f'(r)$  represents the derivative of  $f(r)$  in relation to radius  $r$  of the transformed space. For simplicity

without losing generality, we consider a two-dimensional (2D) optical device and focus our attention on the transverse electric (TE) polarization mode, in which the incident electric field is polarized along the  $z$ -axis and only the  $\mu_r$ ,  $\mu_\phi$ , and  $\varepsilon_z$  components of the material parameters are relevant. Since the simulation can be done in a similar manner for transverse magnetic polarization, the simulation results are not included here for brevity.

Figure 1 shows a schematic diagram of the proposed optical device, where three concentric circles with radii of  $b$ ,  $c$ , and  $d$  divide the transformed space into three regions: the inner region I ( $0 < r < b$ ), the folding region II ( $b < r < c$ ), and the outer region III ( $c < r < d$ ). To design such a device, two-step coordinate transformation is conducted simultaneously along the radial direction. Firstly, the region  $a < r' < b$  in the original space is folded into the region  $b < r < c$  in the transformed space. The inner boundary  $r=r'=b$  and outer boundary  $r=r'=d$  are left unchanged.  $r$  and  $r'$  represent the radii of the transformed and original spaces, respectively. These steps lead to the following boundary conditions:  $f_{\text{II}}(b) = b$ ,  $f_{\text{II}}(c) = a$  for the folding region and  $f_{\text{III}}(d) = d$ ,  $f_{\text{III}}(c) = a$  for the outer region. Assuming that the transformation equations for both regions are linear functions and using the aforementioned boundary conditions as bases, the transformation equations can be expressed as

$$r' = f_{\text{II}}(r) = \frac{b-a}{b-c}(r-b) + b \quad \text{for region II,} \quad (2)$$

$$r' = f_{\text{III}}(r) = \frac{d-a}{d-c}(r-d) + d \quad \text{for region III.} \quad (3)$$

Substituting Eqs. (2) and (3) into Eq. (1), the permittivity and permeability for regions II and III can be easily obtained as

$$\mu_r^{\text{II}} = 1 - \frac{(a-c)b}{(a-b)r}, \quad \mu_\phi^{\text{II}} = \frac{r}{r - \frac{(a-c)}{a-b}b},$$

$$\varepsilon_z^{\text{II}} = \left(\frac{b-a}{b-c}\right)^2 + \frac{(a-c)(b-a)b}{(b-c)^2 r} \quad \text{for region II,} \quad (4)$$

$$\mu_r^{\text{III}} = 1 - \frac{(a-c)d}{(a-d)r}, \quad \mu_\phi^{\text{III}} = \frac{r}{r - \frac{(a-c)}{a-d}d},$$

$$\varepsilon_z^{\text{III}} = \left(\frac{d-a}{d-c}\right)^2 + \frac{(a-c)(d-a)d}{(d-c)^2 r} \quad \text{for region III.} \quad (5)$$

Region I is assumed to be free space in this letter. Equations (4) and (5) provide the general expressions of material parameters for the 2D cylindrical optical device. If  $a$  is set to a value greater than zero, the optical device can act as a transparent device that protects equipment, such as an antenna or a radar station, without compromising their performance. If  $a$  is set to zero, the device can behave as both an internal cloak and an external cloak, allowing the hidden object to exchange information with the outside environment and still move freely within the device. An optimal value of  $a$  that is capable of achieving all three functions simultaneously certainly exists, and finding this value is one of our future research goals. Anisotropic and inhomogeneous material parameters shown in Eqs. (4) and (5)

may be simplified by performing coordinate transformation along the orthogonal direction<sup>[11]</sup> or by choosing the appropriate transformation equation<sup>[26]</sup>. An alternating layered structure made up of two isotropic materials<sup>[9]</sup> or transmission line metamaterials<sup>[29]</sup> may also be used. Full-wave simulation is conducted using the commercial software COMSOL to demonstrate the performance of the optical device.

In the simulation, the entire computational domain is surrounded by a perfectly matched layer that absorbs waves propagating outward from the bounded domain. To achieve the function of a transparent device, the geometric parameters of the optical device are set to  $a=0.3$  m,  $b=0.5$  m,  $c=1$  m, and  $d=2$  m. If we set  $a=0$  while maintaining fixed values for all other geometric parameters, the optical device inherits the characteristics of traditional internal and external cloaks, allowing vision and motion capabilities for the hidden object. However, the material parameters resulting from  $a=0$  have singular values, which may limit the device to a single working frequency and degrade its performance at other frequencies. To avoid singularity and maintain optimum performance when the device functions as an internal and external cloak,  $a$  is set to 0.003 m in the simulation. The performance of the optical device is investigated in several aspects.

To explore the transparent performance of the proposed device, the electric field distributions in the vicinity of the optical device under plane and cylindrical wave irradiation are shown in Figs. 2(a) and (b), respectively. In Fig. 2(a), a 0.6-GHz plane wave occurs from left to right. In Fig. 2(b), a 0.6-GHz line source with a current of 0.003 A/m is located at (0, 0) to generate the cylindrical wave. Although the plane wave is distorted in the transformation region, it returns to the original propagation status when it passes through the device (Fig. 2(a)). No undesired reflection is observed because of perfect impedance matching between the device and the surrounding space. Figure 2(b) indicates that the wavefronts of the cylindrical wave can be recovered perfectly when the line source is located at the center of the device. That is to say, the optical device does not affect the propagation of the cylindrical wave and can in fact be used as a transparent radome structure for protecting an antenna system against adverse weather conditions. We used a 2D horn antenna to demonstrate the feasibility of use of the optical device in antenna protection. Figure 2(c) displays the electric field distribution

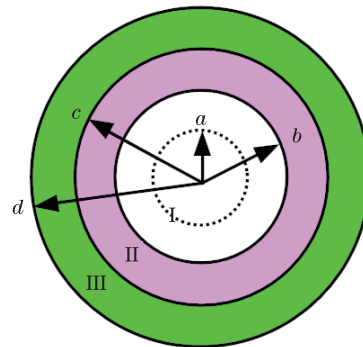


Fig. 1. (Color online) Schematic diagram of the proposed optical device.

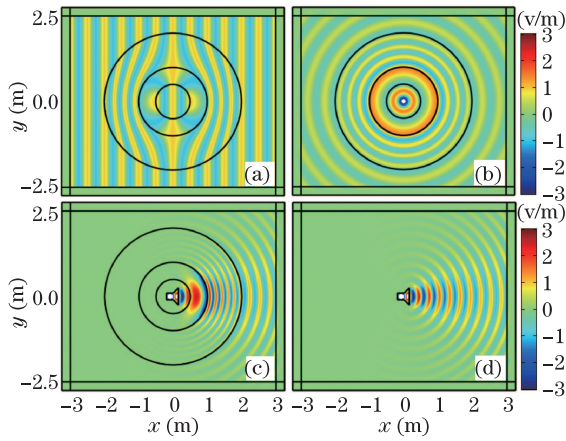


Fig. 2. (Color online) Electric field distribution in the vicinity of the proposed optical device (a) when a plane wave propagates from left to right and (b) when a line source is located at the origin. Electric field distribution of the horn antenna (c) with and (d) without an optical device.

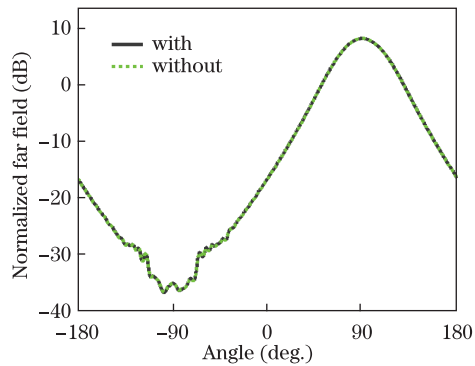


Fig. 3. (Color online) Normalized far field distribution of the horn antenna with and without an optical device.

of a horn antenna covered by the optical device. For comparison, the field distribution of a horn antenna exposed to free space is also simulated, and the results are illustrated in Fig. 2(d). The standing wave in Fig. 2(c), which is caused by strong electromagnetic interactions between the antenna and the device, has no effect on the communication quality of the antenna. Comparing Fig. 2(c) with Fig. 2(d), the field distributions of the horn antenna with and without the optical device in the region of  $r > d$  are evidently the same. To provide a more convincing illustration of the transparent property of the device, the normalized far-field distribution of the horn antenna with and without the optical device is shown in Fig. 3. The far-field distribution of the horn antenna surrounded by the device agrees well with that of the antenna located in free space. Thus, we can conclude that the optical device can be applied as a radome structure.

To validate the vision-enabling property of the optical device when it functions as an internal cloak, we calculate the electric field distribution in the vicinity of the optical device, as illustrated in Fig. 4(a). Figure 4(b) shows the simulation results of a traditional internal cloak. A 0.6-GHz TE-polarized plane wave with unit amplitude impinges from the left-hand side. Figures 4(a) and 4(b) show that the plane wave is smoothly guided around the hidden area for the two kinds of cloaks. The

wavefronts are perfectly restored when the wave exits the cloak, resembling the flow of water around a stone. The incident wave can penetrate through the optical device and encroach on the hidden area, which is impossible for a traditional internal cloak. Further study of this optical device could lead to the development of hidden objects with vision capability. A characteristic feature of the optical device is that it can optically cancel the scattering of hidden objects by utilizing complementary media in the folding region. By contrast, in a traditional internal cloak, a completely enclosed domain is created where the electromagnetic wave does not exist to make objects invisible. Figure 4(c) shows a comparison of electric field distributions along the  $x$ -axis of the hidden area. The electromagnetic wave can enter the hidden area, and the field intensity at the centre is equal to the field intensity of wave transmission in free space. However, no electromagnetic wave exists in the hidden area of a traditional internal cloak, which indicates that an object enclosed by the proposed optical device can have vision capability and receive information from the external environment without distortion, whereas the traditional internal cloak is completely "blind" to the outside environment.

Moving one step further, we examine whether or not the proposed optical device has the ability to render objects invisible when used as an internal cloak. Figure 5(a) displays the scattering pattern of a woman-like rigid scatterer, in which the plane wave occurs horizontally from left to right. The plane wave is strongly disturbed by the rigid scatterer, resulting in a remarkable backward reflection and a sharp-edged shadow. The scattering pattern in the vicinity of the rigid scatterer covered by the optical device is also simulated for comparison, and the results are shown in Fig. 5(b). The white flecks in the figure represent overvalued fields that occur because of surface mode resonance induced by optical cancellation between the scatterer and the complementary media.

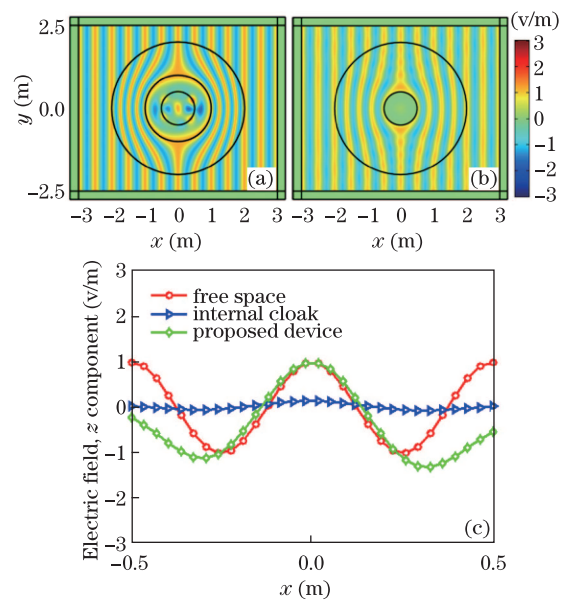


Fig. 4. (Color online) Electric field distribution in the vicinity of (a) the proposed optical device and (b) a traditional internal cloak under plane wave irradiation. (c) Comparison of electric field distributions along the  $x$ -axis of the hidden area.

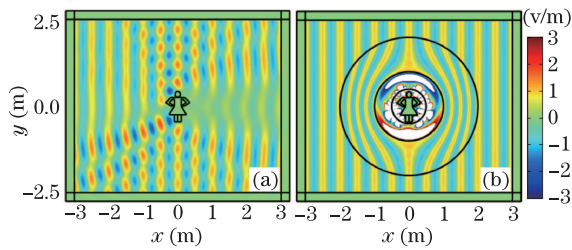


Fig. 5. (Color online) (a) Scattering pattern of a woman-like rigid scatterer. (b) The scatterer in (a) is cloaked by the proposed optical device.

From Fig. 5(b), we can observe that the plane wave is nearly undistorted outside the optical device, almost as if no scatterer is present in the space. Inside the device, the wave is regularly bent around the hidden area but completely restored to the original wavefront when passing through the device. For an exterior observer behind the device, the electromagnetic wave seems to be emitted directly from the source. Therefore, the scatterer is perfectly cloaked. Even arbitrarily shaped objects can be cloaked inside the device, and no geometric or material limitations for hiding objects are observed. The object can be cloaked as long as it fits inside the cylindrical region of  $r < b$ . The cloaking performance of the optical device is independent of incident wavefronts and wave directions. For brevity, the corresponding simulation results are omitted here.

Besides its vision-enabling and object-concealing properties, the optical device can also function as a traditional external cloak and use an anti-object to conceal objects. The underlying mechanism is summarized in the following statements. Firstly, the scatterings of the hidden object and the surrounding space are optically cancelled by a complementary medium embedded with an anti-object in the folding region. Then, the correct optical path in the cancelled space is restored by the outer region. Figure 6(a) portrays the scattering pattern of a curved sheet with a thickness of 0.2 m and a relative permittivity of  $\epsilon_r = 3 + j0.001$ . To enable invisibility, we include a custom-made anti-object with material parameters of  $\epsilon' = (3 + j0.001)\epsilon^{\text{II}}$  and  $\mu' = \mu^{\text{II}}$  in the folding region of the optical device, as illustrated in Fig. 6(b). Figure 6(d) shows the scattering pattern of a curved sheet with a thickness and material parameters identical to those of the sheet in Fig. 6(a). Figure 6(e) shows the cloaking effect of a sheet cloaked by a traditional external cloak. The perfectly recovered wavefronts of the impinging plane wave shown in Figs. 6(b) and 6(e) clearly demonstrate the perfect cloaking capabilities of the proposed optical device and the traditional external cloak for the two curved sheets. Moreover, for the optical device, no strict requirement in terms of the positions of the hidden object and anti-object is observed, and the hidden object is allowed more freedom of movement in its position. Figure 6(c) shows the electric field distribution in the vicinity of a curved sheet cloaked by the optical device with a rotation offset of  $45^\circ$  between the curved sheet and the anti-object. Figure 6(c) demonstrates that the optical device performs well even with the offset. For the traditional external cloak, the scattered fields are dramatically enhanced when the positions of the hid-

den object and the anti-object exhibit a small rotation offset of  $1^\circ$ , as shown in Fig. 6(f). The optical device can thus be concluded to function as a traditional external cloak while enabling movement within the device.

Finally, the effect of material loss on the performance of the optical device is studied, as loss of artificial metamaterials is always possible in practical applications. Four cases with electric and magnetic loss tangents ( $\text{tg}\delta$ ) of 0.001, 0.005, 0.01, and 0.015 are considered. Figures 7(a)–(d) show the cloaking effect of the curved sheet for these four cases. Figures 7(a) and 7(b) indicate that the field patterns are basically undisturbed and the device effectively conceals the sheet for metamaterials with  $\text{tg}\delta$  of 0.001 and 0.005. However, when the  $\text{tg}\delta$  of metamaterials is 0.01 or greater, forward scattering may be observed (Figs. 7(c) and 7(d)). Thus, metamaterial  $\text{tg}\delta$  of less than 0.01 are acceptable.

In conclusion, an optical device with three functions based on two-step coordinate transformation has been proposed. Apart from its function as a transparent device,

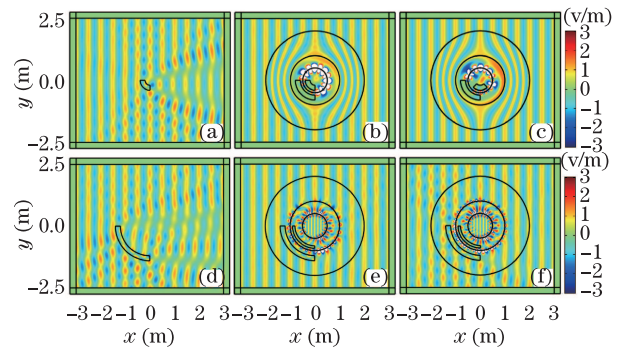


Fig. 6. (Color online) (a) Scattering pattern of a curved sheet with a thickness of 0.2 m and relative permittivity of  $\epsilon_r = 3 + j0.001$ . (b) Cloaking effect of the curved sheet in (a) covered by the proposed optical device when the positions of the hidden object and the anti-object possess a rotation offset of  $0^\circ$  and (c)  $45^\circ$ . (d) Scattering pattern of a curved sheet with the same thickness and material parameters as the sheet in (a). (e) Cloaking effect of the curved sheet in (d) covered by a traditional external cloak when the positions of the hidden object and the anti-object possess a rotation offset of  $0^\circ$  and (f)  $1^\circ$ .

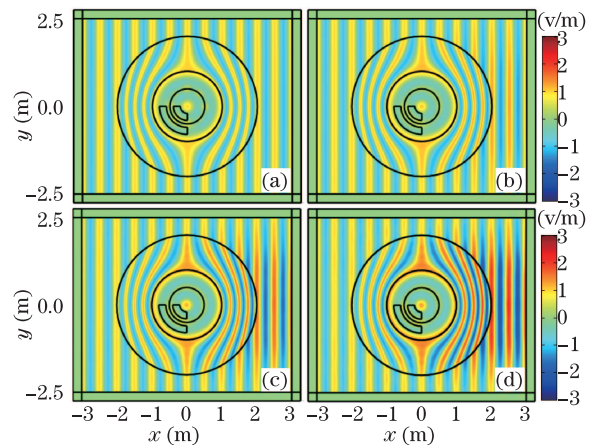


Fig. 7. (Color online) Electric field distribution of a curved sheet covered by the proposed optical device with loss tangents of (a) 0.001, (b) 0.005, (c) 0.01, and (d) 0.015.

the device has the characteristic features of traditional internal and external cloaks. The proposed optical device also enables vision and movement capability for enclosed objects. The general permittivity and permeability of the device are derived, and the performance of device is validated by full-wave simulation. Results show that the device performs well for each function, and that metamaterials with  $\text{tg}\delta$  of less than 0.01 have little influence on the performance of device. The device discussed here is limited to a 2D case, but the same strategies can be applied for the analysis of a more complex three-dimensional (3D) case. Our results can be used for designing more compact optical devices and contributes to the development of new applications in the electromagnetics industry.

This work was supported by the National Natural Science Foundations of China (Nos.61161007 and 61261002), the Scientific Research Fund Major Project of the Education Bureau of Yunnan Province (No. ZD2011003), the Natural Science Foundation of Yunnan Province (No. 2011FB018), and the Doctoral Program of Higher Education (No. 20125301120009).

## References

1. J. B. Pendry, D. Schurig, and D. R. Smith, *Science* **312**, 1780 (2006).
2. U. Leonhardt, *Science* **312**, 1777 (2006).
3. E. E. Narimanov and A. V. Kildishev, *Appl. Phys. Lett.* **95**, 041106 (2009).
4. W. X. Jiang, J. Y. Chin, and T. J. Cui, *Mater. Today* **12**, 26 (2009).
5. H. Y. Chen, C. T. Chan, and P. Sheng, *Nat. Mater.* **9**, 387 (2010).
6. N. B. Kundtz, D. R. Smith, and J. B. Pendry, *Proc. IEEE* **99**, 1622 (2011).
7. D. Schurig, J. J. Mock, B. J. Justice, S. A. Cummer, J. B. Pendry, A. F. Starr, and D. R. Smith, *Science* **314**, 977 (2006).
8. W. S. Cai, U. K. Chettiar, A. V. Kildishev, V. M. Shalaev, and G. W. Milton, *Appl. Phys. Lett.* **91**, 111105 (2007).
9. Y. Huang, Y. J. Feng, and T. Jiang, *Opt. Express* **15**, 11133 (2007).
10. C. Li and F. Li, *Opt. Express* **16**, 13414 (2008).
11. W. Li, J. Guan, Z. Sun, W. Wang, and Q. Zhang, *Opt. Express* **17**, 23410 (2009).
12. Y. Lai, H. Chen, Z. Zhang, and C. Chan, *Phys. Rev. Lett.* **102**, 093901 (2009).
13. C. Yang, J. Yang, M. Huang, Z. Xiao, and J. Peng, *Opt. Express* **19**, 1147 (2011).
14. M. W. McCall, A. Favaro, P. Kinsler, and A. Boardman, *J. Opt.* **13**, 024003 (2011).
15. J. Yang, M. Huang, C. Yang, and J. Yu, *Eur. Phys. J. D* **61**, 731 (2011).
16. H. Chen and C. Chan, *Appl. Phys. Lett.* **90**, 241105 (2007).
17. W. Wang, L. Lin, X. Yang, J. Cui, C. Du, and X. Luo, *Opt. Express* **16**, 8094 (2008).
18. Z. Chen, L. Wang, C. Wang, and Z. Fang, *Chin. Opt. Lett.* **9**, 021601 (2011).
19. T. Li, M. Huang, J. Yang, J. Yu, and Y. Lan, *J. Phys. D: Appl. Phys.* **44**, 325102 (2011).
20. V. Giniis, P. Tassin, J. Danckaert, C. M. Soukoulis, and I. Veretennicoff, *New J. Phys.* **14**, 033007 (2012).
21. H. Chen and C. Chan, *J. Phys. D: Appl. Phys.* **43**, 113001 (2010).
22. Z. Chang, J. Hu, G. Hu, R. Tao, and Y. Wang, *Appl. Phys. Lett.* **98**, 121904 (2011).
23. W. Zhu, I. D. Rukhlenko, and M. Premaratne, *J. Opt. Soc. Am. B* **29**, 2659 (2012).
24. S. Guenneau, C. Amra, and D. Veynante, *Opt. Express* **20**, 8207 (2012).
25. T. Zentgraf, J. Valentine, N. Tapia, J. Li, and X. Zhang, *Adv. Mater.* **22**, 2561 (2010).
26. J. S. Mei, Q. Wu, and K. Zhang, *Chin. Opt. Lett.* **10**, 071605 (2012).
27. T. Y. Huang, H. C. Lee, I. W. Un, and T. J. Yen, *Appl. Phys. Lett.* **101**, 151901 (2012).
28. U. Leonhardt and T. G. Philbin, *New J. Phys.* **8**, 247 (2006).
29. C. Li, X. Liu, and F. Li, *Phys. Rev. B* **81**, 115133 (2010).